Sedimentary Geology 296 (2013) 21–35

Contents lists available at ScienceDirect

Sedimentary Geology

journal homepage: www.elsevier.com/locate/sedgeo

High-resolution sequence stratigraphy and continental environmental evolution: An example from east-central Argentina

Elisa Beilinson *, Gonzalo D. Veiga, Luis A. Spalletti

Centro de Investigaciones Geológicas (Consejo Nacional de Investigaciones Científicas y Técnicas — Universidad Nacional de La Plata), Calle 1 No. 644 (B1900TAC) La Plata, Argentina

ARTICLE INFO

Article history:
Received 30 April 2013
Received in revised form 7 August 2013
Accepted 8 August 2013
Available online 17 August 2013

Editor: J. Knight

Keywords:
Allogenic controls
Sequence stratigraphy
Plio-Pleistocene
Argentina
Fluvial systems

ABSTRACT

The aims of this contribution is to establish a high-resolution sequence stratigraphic scheme for the continental deposits that constitute the Punta San Andrés Alloformation (Plio-Pleistocene) in east-central Argentina, to analyze the basin fill evolution and to identify and assess the role that extrinsic factors such as climate and sea-level oscillations played during evolution of the unit.

For the high-resolution sequence stratigraphical study of the Punta San Andrés Alloformation, high- and low-accommodation system tracts were defined mainly on the basis of the architectural elements present in the succession, also taking into account the relative degree of channel and floodplain deposits. Discontinuities and the nature of depositional systems generated during variations in accommodation helped identify two fourth-order high-accommodation system tracts and two fourth-order low-accommodation system tracts. At a third-order scale, the Punta San Andrés Alloformation may be interpreted as the progradation of continental depositional systems, characterized by a braided system in the proximal areas, and a low-sinuosity, single-channel system in the distal areas, defined by a high rate of sediment supply and discharge peaks which periodically flooded the plains and generated high aggradation rates during the late Pliocene and lower Pleistocene.

1. Introduction

Many studies of late Cenozoic climate and sea level change emphasize their extreme glacial or interglacial character. However, oxygen isotope curves (Imbrie et al., 1984; Chappell and Shackleton, 1986; Williams et al., 1988; Waelbroeck et al., 2002) show that approximately 80% of the glacial cycles during the middle and late Pleistocene shows intermediate characteristics, with minimum temperatures below those of interglacial periods, but not as cold as those of full glacials. Likewise, the decrease in glaci-eustatic sea-level, estimated between 100 and 140 m for a full glacial event (Clapperton, 1993; Rabassa et al., 2005; Rabassa and Coronato, 2009), may have been between 40 and 85 m for these intermediate situations. These multiple late Cenozoic climate variations triggered cycles of glaciation/interglaciation in Patagonia that led to sudden changes in sediment supply, fluvial discharge and sea level (Cavallotto and Violante, 2005).

The Punta San Andrés Alloformation (PSAA) comprises a classical Plio-Pleistocene continental sedimentary succession of the Argentinian Pampean Plain (Fig. 1) that accumulated contemporaneously with Patagonian glaciations. The Punta San Andrés Alloformation has been studied since the early 1900s because of its rich vertebrate fauna. It comprises up to 18 m of very well-exposed sedimentary rocks that display several palaeosols stacked among alluvial and fluvial deposits.

The PSAA provides a unique opportunity for high-resolution analysis of the role that climate and glacio-eustasy played in the evolution of continental depositional systems. This work aims at: a) building a general sequence stratigraphic framework for this unit on the basis of lateral and vertical variations of sedimentary facies and palaeosols, system tract stratigraphic bounding surfaces, and b) identifying and assessing the role that extrinsic factors such as climate and glacio-eustatic sea-level oscillations played during evolution of the unit.

2. Geological setting

The late Cenozoic Pampean basins (Fig. 1a) are part of the extra-Andean foreland region of central Argentina and are bounded to the east by the Atlantic passive margin and to the west by the Andean deformational front. The accumulation of post-Miocene deposits in the Pampean region (Fig. 1a), near the passive margin, was favored by high sediment availability, associated with the rise of the Andean Cordillera (Turic et al., 1996; Parker et al., 2008). On the Argentinian coastline, tectonic or neotectonic activity has been scarce and the development of marine cliffs is related to uplift by lithostatic rebound (Folguera and Zárate, 2011; Pedoja et al., 2011). On the Bonaerenian coast (Fig. 1a), the estimated uplift rate for the last 100 kyr is of 0.01 to 0.03 mm/year (Pedoja et al., 2011). This rate could explain the 12 to 18 m-high marine cliffs in the study area but cannot be extrapolated to the rest of the Pleistocene or be taken into account as a driving factor in the Punta San Andrés Alloformation deposition.

* Corresponding author. Fax: +54 221 4215677.
E-mail address: beilinson@cig.museo.unlp.edu.ar (E. Beilinson).

0037-0738/$ – see front matter © 2013 Elsevier B.V. All rights reserved.
http://dx.doi.org/10.1016/j.sedgeo.2013.08.008

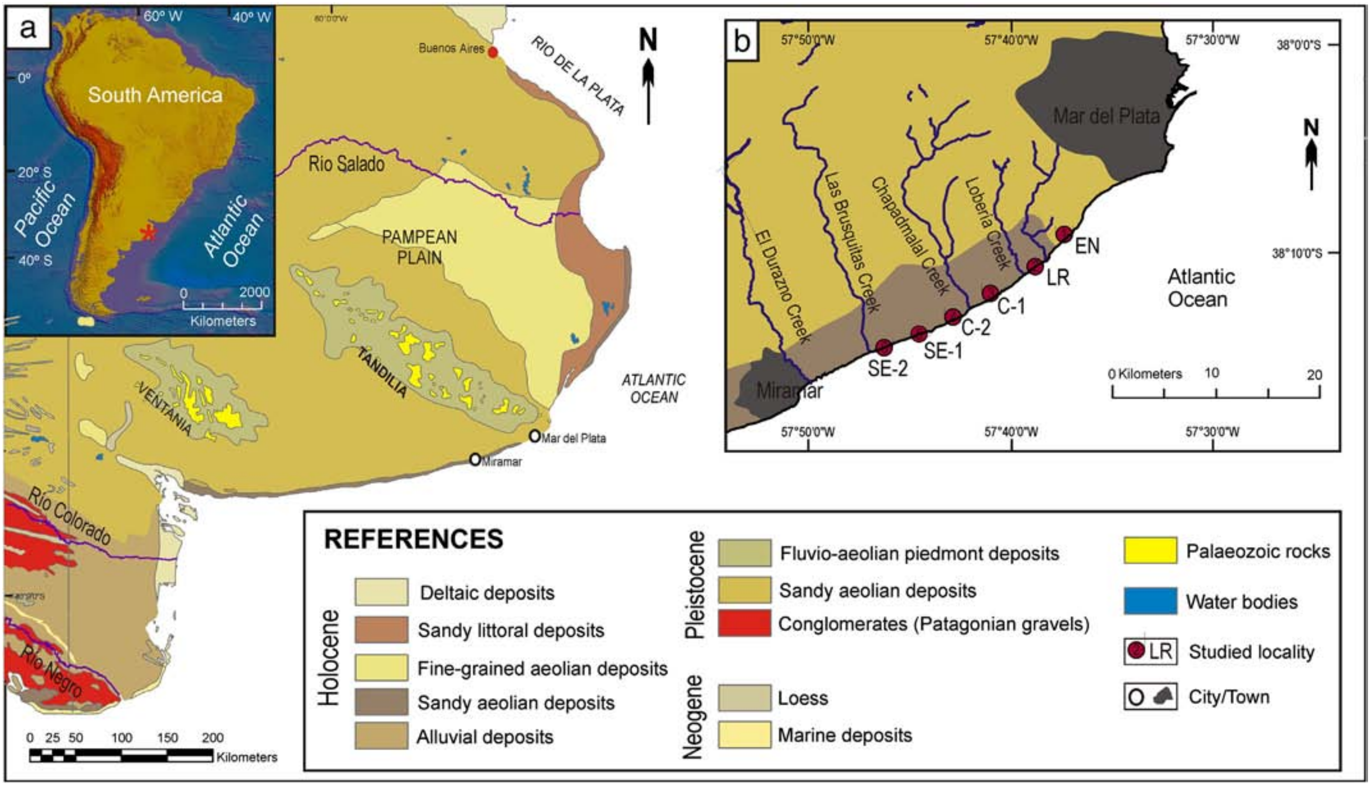

Fig. 1. a) Regional setting of the study area and b) location of the main sites.

In the east-central Pampean region, the late Cenozoic succession comprises a series of Plio-Pleistocene continental deposits capped by an extensive plateau of loess and loess-like deposits of late Pleistocene and Holocene age. The study area is located in the south-eastern margin of the Tandilia Range, a succession of hills and mountains with a NW–SE trend spanning 350 km in length and 60 km maximum width (Fig. 1a). The studied unit crops out in the coastal cliffs of east-central Buenos Aires province between the cities of Mar del Plata and Miramar (Fig. 1b).

The Punta San Andrés Alloformation deposits were assigned to the late Pliocene–late Pleistocene and they comprise a continental succession of fluvial, lacustrine and loess-like facies (Zárate, 1989; Beilinson, 2009, 2011). The base of this unit is in sharp contact with Pliocene mudstones of the Punta Martínez de Hoz Alloformation and its top is represented by late Pleistocene–Holocene psammitic deposits of the Arroyo Lobería Alloformation (Fig. 2). The thickness of the Punta San Andrés Alloformation ranges between 12 and 18 m. The unit consists

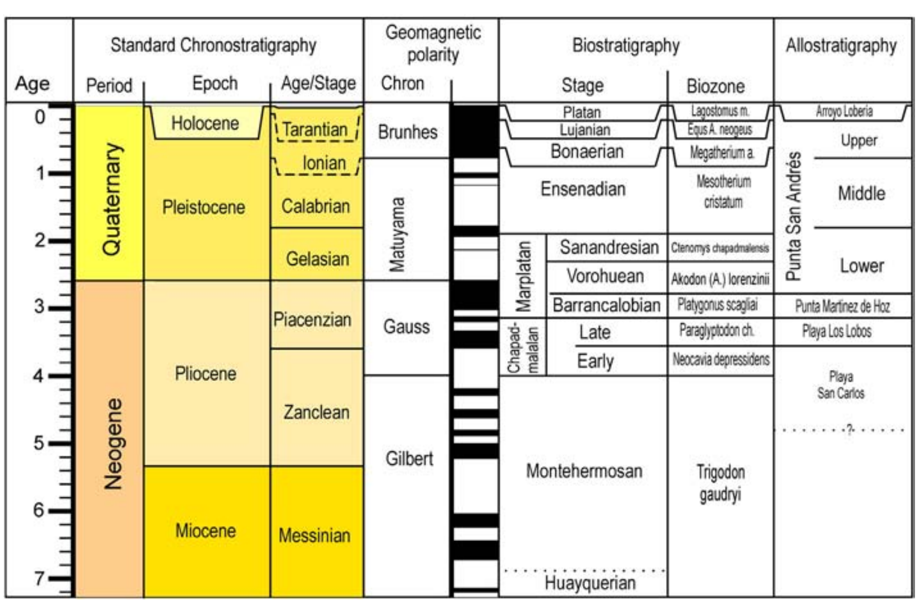

Fig. 2. Stratigraphic chart including biostratigraphic units by Cione and Tonni (2005) and allostratigraphic units by Zárate (1989).

of sandstones, silty sandstones and sandy mudstones, with variable development of vertic and calcic palaeosols. The presence of reworked pyroclastic materials in the studied deposits is considered evidence of contemporaneity of deposition with explosive volcanic events in the Andes or the recycling of Patagonian pyroclastic deposits (Teruggi et al., 1957).

The rich vertebrate fauna present in this and related units has been the basis for the South American Late Cenozoic biostratigraphic zonation (Marshall, 1985; Cione and Tonni, 1995, 1999, 2005) (Fig. 2). Trace fossils are also abundant, the most common being related to invertebrate activity (Beilinson and Taglioretti, 2013).

Although the PSAA lacks isotopic data for a precise age determination, some age approximations can still be made. The Punta Martínez de Hoz Alloformation deposits, which are immediately below the studied unit, contain vesicular impact glasses with an $^{40}Ar/^{39}Ar$ age of 3.27 ± 0.08 Ma (Schultz et al., 1998). Based on stratigraphic relationships with the adjacent units, the PSAA broadly spans the late Pliocene to late Pleistocene (Zárate, 1989, 2005). Palaeomagnetic polarity and biostratigraphy have further allowed subdivision of the deposits into three informal allomembers (Zárate, 1989) (Fig. 2).

3. Methodology

Due to the physiographic nature of the coastal cliffs, a large part of them is inaccessible. As such, in order to study the relationships between the different sandbodies, photomosaics were made from a boat, with field work carried out wherever possible. The sedimentological and palaeopedological data were collected from 6 selected localities (Fig. 1b), which were the ones that provided the best accessibility and displayed important lithological and architectural variations.

In each locality, a detailed sedimentological log was made, registering grain-size, primary sedimentary structures, palaeocurrents, nature of discontinuities, scale and geometry of lithosomes, palaeopedological features, degree of bioturbation and fossil content. Sedimentary facies were described according to Miall's (1978, 2006) scheme. The architectural elements and the hierarchy of the bounding surfaces were defined according to Miall (2006). Samples were collected for petrographical analysis and for micromorphological features of the palaeosols. The latter was carried out using the terminology suggested by Bullock et al. (1985). Since many of the critical features for classifying modern soils (*i.e.*, cation exchange capacity, moisture regime, bulk density, etc) do not survive into the rock record, Mack et al.'s (1993) classification for palaeosols was used herein. This scheme utilizes those pedofeatures with the highest preservation potential in the rock record such as organic matter content, horizonation, redox condition, illuviation of insoluble minerals and accumulation of soluble minerals.

The mineralogy of the <4 μm fraction of the palaeosols was determined by X-ray diffraction (XRD). Semi-quantitative estimates of the relative concentrations of clay minerals were based on the peak area method (Biscaye, 1965) on glycolated samples. Relative percentages of each clay mineral were determined by applying empirical factors (Moore and Reynolds, 1989). The abundance of different clay minerals in the <4 μm fraction and the palaeopedological features identified in the Punta San Andrés deposits are summarized in Table 1.

Table 2
Facies of the Punta San Andrés Alloformation.

Facies	Features	Interpretation
Gmg	Matrix-supported gravel, crudely bedded with normal grading. Medium to fine sandstone matrix. Clasts of micrite and/or Fl, Fm facies. Tabular bodies with erosive base.	Pseudoplastic debris flow
Gh	Clast-supported gravel with normal grading. Lenticular to tabular bodies with erosive base.	Longitudinal bedforms; lag deposits
Gt	Gravel — very coarse sandstone with trough cross-bedding. Cosets of 100–150 cm.	Channel-fill deposits; sinuous-crested (3D) dunes.
St	Fine to medium sandstone, sometimes pebbly. Trough cross-bedding.	Sinuous-crested and linguidis (3D) dunes
Sp	Fine to medium sandstone; silty sandstone. Planar cross-bedding. Tabular to concave-up based bodies with flat tops.	Transverse (2D) dunes
Sh	Fine to medium sandstone; silty sandstone. Horizontal bedding. Tabular bodies with erosive base.	Sheet flows; plane-bed flow
Sm	Fine silty to medium sandstone. Massive or with faint lamination. Tabular bodies.	Plane-bed flow (lower flow regime)
Fl	Interlamination of siltstone and very fine sandstone.	Deposition from suspension and from weak traction currents.
Fm	Mudstone and siltstone. Massive or with faint lamination. Sometimes with desiccation cracks. Tabular bodies.	Suspension fallout in still water

4. Sedimentological and palaeoenvironmental analysis

4.1. Description and interpretation of architectural elements

Five genetically significant architectural elements were identified with the aid of facies associations (Table 2), geometry, palaeocurrents, unit dimensions and determination of the hierarchy of the bounding surfaces (Table 3). The sediment bodies are mainly ribbon-shaped and sheet-like in geometry. The dominant lithologies in order of decreasing abundance are fine to medium sandstone, fine conglomerate with sandy matrix, sand–mud heteroliths and intraformational calcirudite.

4.1.1. Architectural element 1 (AE 1): multistory fluvial channels

4.1.1.1. Description. Multistory sand-dominated bodies with narrow sheet geometry (*sensu* Gibling, 2006) commonly occur in the upper PSAA. These bodies are between 25 and 90 m wide and 1.5 and 3 m thick [width/thickness (W/T): 16–30] and are incised in the underlying fine-grained deposits. The AE 1 bodies are characterized by a single basal erosion surface that shows up to 5 m of relief and internally

Table 1
Pedofeatures and average composition of the <4 μm fraction in the Punta San Andrés Alloformation palaeosols. Sm: smectite; K: kaolinite; I: illite; Ch: chlorite; I–S: interstratified illite–smectite: C–S: interstratified chlorite–smectite; K–S: interstratified kaolinite–smectite; x: absent; s: scarce; c: common; tr: traces.

Palaeosol	Pedofeatures		Average composition of the <4 mm fraction						
	Mesofeatures	Microfeatures	% I	% Sm	% K	% Ch	I/S	C/S	K/S
Vertisols	Slickensides, pseudoanticlines, desiccation cracks	Fe-nodules (0.2–0.5 mm), evidence of root activity, clay coatings and hypo-coatings, subangular blocky peds, porostriated and granostriated b-fabric	56.7	27.7	10.8	4.8	c	c	tr
Calcisol	Morphologies stage II to VI: nodular, laminar and massive carbonates	Micrite with floating etched detrital grains, alveolar-septal structure	57	23.3	12.6	6.6	c	s	s
Protosols	Discrete carbonate nodules and/or glaebules, poor horizonation	Evidence of root activity, weakly developed peds	9	40.5	49.3	–	c	x	tr

Table 3
Architectural elements of the Punta San Andrés Alloformation.

Architectural element	Principal facies assemblage	Geometry and relationships	Interpretation
AE 1 (multistory fluvial channels)	Gh, Gt, St, Sm, Sp	Sandbodies with concave-up to irregular erosional base (5th order surface) and sheet geometry (W/T: 15–35); internally 3 to 4 laterally shifted stories. Paleocurrents: S–SE with low dispersion. Internal concave-up and lateral-accretion 3rd order surfaces.	Low-sinuosity, fixed channel deposits
AE 2 (single fluvial channels)	Gmg or Gh, St, Sm	Single symmetric ribbon sandbodies (W/T < 3.5) with low relief basal erosion surface (4th order surface). Encased in fine-grained deposits. Characteristic absence of lateral accretion surfaces. Paleocurrents: N–NW with low dispersion	Minor floodplain channels; crevasse-channel deposits
AE 3 (flash flood deposits)	Gmg; Sh, Sm	Erosionally based tabular bodies (0.1–0.2 m thick, 10s of meters wide) stacked in 0.8–1.2 m successions. General arrangement of the beds is finning-upward. Internal arrangement is chaotic to normally graded. No bioturbation observed.	Mantiform flash flood events related to episodical overbank flows and flooding of the proximal floodplain
AE 4 (proximal floodplain deposits)	Sh, Fl, Sm	Erosionally based (4th order surface) wedge-like bodies with flat to convex tops. Deposits are sparsely bioturbated. General arrangement of the beds is coarsening-upward but internally each bed fines upward.	Crevasse-splay deposits related to avulsion processes; inmature paleosols
AE 5 (distal floodplain deposits)	Fl, Sm, Fm	Tabular beds (0.8–2 m thick, hundreds of meters wide) with a 4th order basal surface. Abundant pedogenic features such as vertical root traces, mottling, slickensides and abundant calcium carbonate deposits. Trace fossils are common within beds in the form of vertical, cylindrical, unlined and lined, passively filled tubes. Pervasive bioturbation is common in some beds.	Deposition is related to suspension fallout in very shallow-water or isolated ephemeral ponds associated with flooding events in the distal floodplain. Abundance of pedogenic and biogenic processes.

comprise 3 to 4 laterally-shifted, vertically stacked stories (Fig. 3a). These bodies rarely present lateral accretion surfaces. The story units are bounded by scour surfaces and internally display a weak fining-upward trend. They show unimodal palaeocurrent directions to the S–SE with low dispersion. The AE 1 bodies mostly comprise clast-supported conglomerates with trough cross-bedding and/or normal grading (Fig. 3b–d), trough cross-bedded pebbly sandstones (Fig. 3e), fine- to medium-grained sands with planar or low-angle cross-bedding (Fig. 3f) and massive to faintly laminated silty sands.

4.1.1.2. Interpretation. The AE 1 deposits are mainly related to fluvial in-channel processes such as the migration of 2D or sinuous-crested (3D) dunes or as lag deposits (Clemente and Pérez-Arlucea, 1993; García-Gil, 1993; Ghosh et al., 2006; Miall, 2006). The low palaeocurrent variability and rarity of lateral accretion surfaces indicates transport by high-energy currents and suggests the presence of low sinuosity, fixed channels (Miall, 2006). Convex-upward, large-scale inclined surfaces (Fig. 3g) point to diversion of flow and presence of braided rivers (Paredes et al., 2007).

4.1.2. Architectural element 2 (AE 2): single fluvial channels

4.1.2.1. Description. These single-story sand bodies display a ribbon geometry and occur in the lower and middle PSAA. They range from 1 to 7 m wide and 0.9 to 2 m thick (W/T < 3.5) and they are commonly incised in the underlying fine-grained deposits. They occur encased within siltstones and mudstones (1 to 2 m thick). The AE 2 bodies have a single concave upwards basal surface with up to 2 m of relief and no internal major bounding surfaces (Fig. 4a,b). They show unimodal palaeocurrent directions to the N–NW with low dispersion. There are two main types of in fill: a chaotic, coarser one composed of crudely bedded matrix-supported conglomerates with normal grading (Fig. 4a), and a finer one characterized by clast-supported conglomerates with normal grading, trough cross-bedded pebbly sandstones and massive to faintly laminated silty sandstones (Fig. 4b).

4.1.2.2. Interpretation. The chaotic AE 2 deposits are interpreted as the result of pseudoplastic debris flows (Miall, 2006). The sandy deposits are related to fluid high-energy currents with in-channel tractive processes such as the migration of 2D and 3D dunes (Clemente and Pérez-Arlucea, 1993; Miall, 2006). These sand ribbons encased within fine-grained deposits are interpreted as straight fluvial channels or crevasse-channels that were in filled during single episodes of deposition (Ghosh et al., 2006).

4.1.3. Architectural element 3 (AE 3): flash flood deposits

4.1.3.1. Description. This architectural element is characterized by tabular pebbly sand bodies that commonly occur in the middle and upper PSAA. These bodies are 0.2 to 2 m thick and several tens of meters wide and are vertically stacked in 0.8 to 1.2 m successions. These bodies have a planar erosive basal surface. They mostly comprise crudely bedded matrix-supported conglomerates with normal grading (Fig. 4c), fine- to medium-grained sands with horizontal bedding (Fig. 4d) and massive to faintly laminated silty sands (Fig. 4e). No palaeocurrent measurements could be obtained from these levels and no bioturbation was observed.

4.1.3.2. Interpretation. AE 3 lithosomes are related to flash floods related to episodic overbank flows and flooding of the proximal floodplain (North and Davidson, 2012).

4.1.4. Architectural element 4 (AE 4): proximal floodplain deposits

4.1.4.1. Description. The AE 4 bodies are composed by individual sheets that are generally 0.6–0.8 m thick and that expand laterally for tens of meters (Fig. 4f). They characterize the lower and middle PSAA. Individual bodies thin distally and have sharp and planar basal contacts. These lithosomes are dominated by silty sands with parallel to low-angle stratification and interlaminated silts and very fine sands (Fig. 4g) or by fine silty sands, massive or with faint lamination. Internally each sheet body fines upwards but the general stacking pattern of the complex is coarsening-upwards. Some poorly developed palaeosols occur in these sheet complexes (see Section 4.2.).

4.1.4.2. Interpretation. The occurrence of parallel to low-angle stratification and the sharp and planar nature of the lower and upper contacts of the AE 4 individual sand bodies suggest emplacement from poorly confined ephemeral flows (Ghosh et al., 2006). Deposition occurred at dune to upper stage flow conditions (Miall, 2006). The massive silty sand sheets also indicate rapid deposition. In spite of lacking physical connection between these bodies and channel-fill deposits, AE 4 sheet

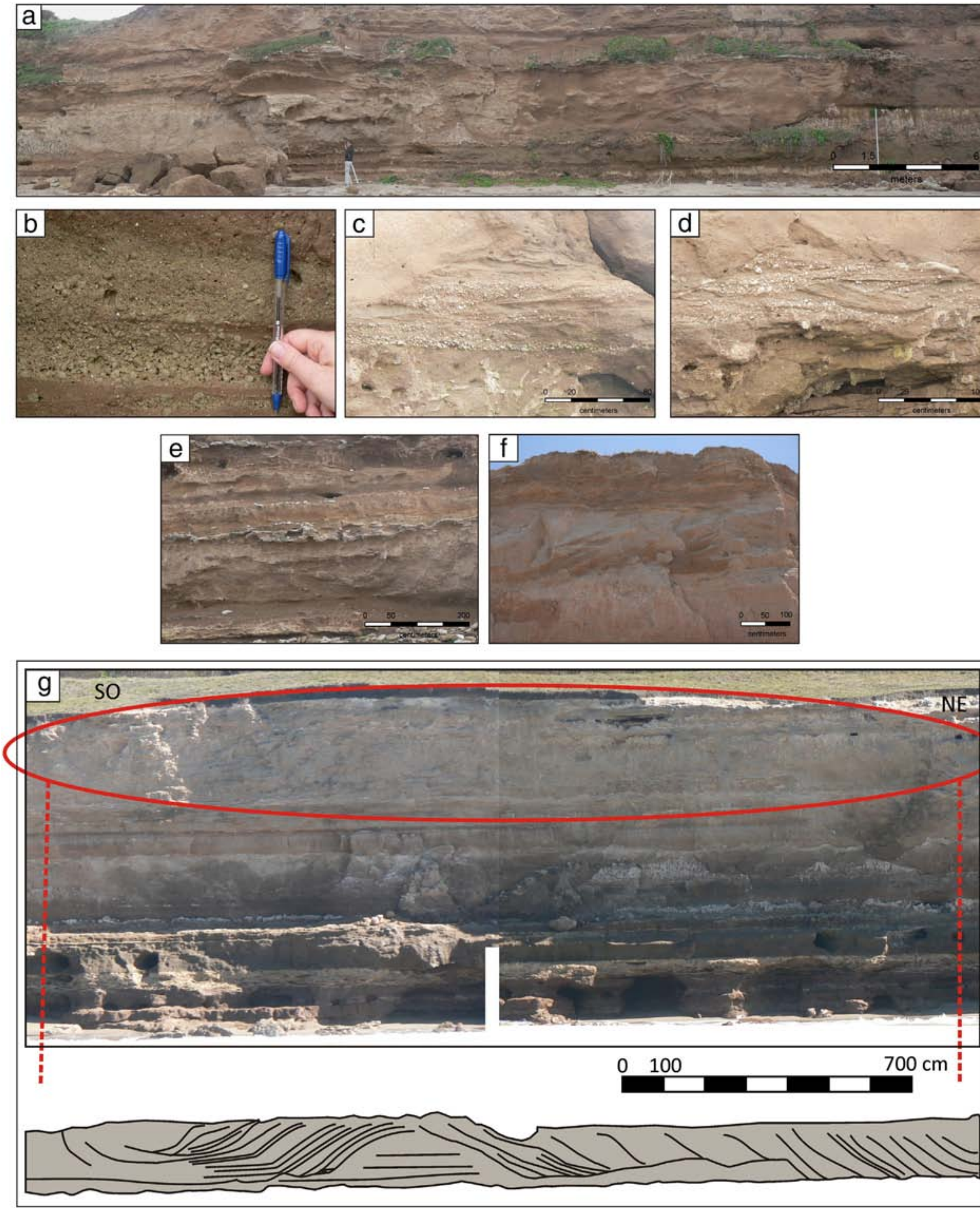

Fig. 3. Architectural elements and sedimentary facies of Punta San Andrés Alloformation. a) AE 1 bodies showing a single basal erosion surface and internally comprise 3 to 4 laterally-shifted stories; b and c) Gh facies: clast-supported gravels with normal grading; d) Gt facies: clast-supported gravels with trough cross-bedding; e) St facies: trough cross-bedded pebbly sands; f) Sp facies: fine- to medium-grained sands with planar or low-angle cross-bedding; g) convex-upward, large scale, inclined surfaces in AE 1 sand bodies points to the diversion of the flow and presence of braided rivers.

complexes are interpreted as crevasse-splay deposits (Ghosh et al., 2006; Smith and Pérez-Arlucea, 2008).

4.1.5. Architectural element 5 (AE 5): distal floodplain deposits

4.1.5.1. Description. This architectural element commonly occurs in the lower and middle PSSA and is dominated by brownish interlaminations of silts and very fine sands and by massive muds and silts with desiccation cracks (Fig. 4h). These lithosomes constitute tabular beds that are 0.8 to 2 m thick and hundreds of m wide (Fig. 4i) and show abundant vertic and calcic pedogenic features (see Section 4.2.). Trace fossils are common and are assigned to *Taenidium serpentinum* and *Beaconites coronus* (Beilinson and Taglioretti, 2013). Pervasive bioturbation is common locally.

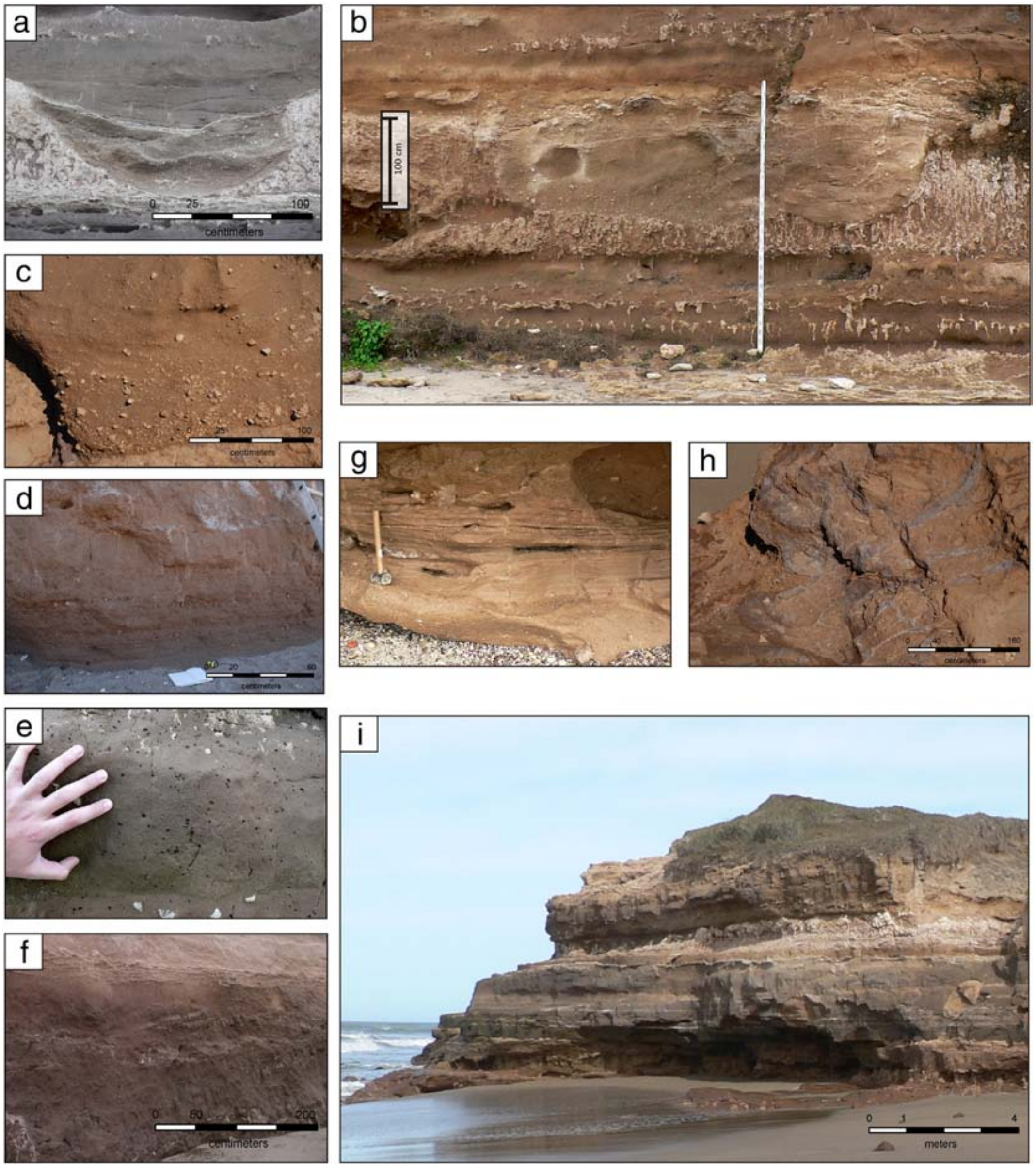

Fig. 4. Architectural elements and sedimentary facies of Punta San Andrés Alloformation. a) AE 2 bodies with no internal major bounding surfaces and chaotic in fill; b) AE 2 bodies characterized by clast-supported conglomerates, trough cross-bedded pebbly sands and massive to faintly laminated silty sands; c) matrix-supported conglomerates with normal grading; d) fine- to medium-grained sands with horizontal bedding; e) massive to faintly laminated silty sandstones; f) AE 4 bodies composed by individual sand sheets; g) AE 4 lithosomes dominated by silty sands; h) interlaminations of silts and muds with desiccation cracks; i) AE 5 tabular bodies.

4.1.5.2. Interpretation. The interlaminated and massive muds and silts are linked to deposition from suspension in weak traction currents or suspension fall-out in still water bodies (Ghosh et al., 2006). As such, they are related to shallow water or isolated ephemeral ponds associated with flooding events on the distal floodplain (Abdul Aziz et al., 2003).

4.2. Palaeosols

One distinctive characteristic of the Punta San Andrés Alloformation is the presence of palaeosols. They constitute continuous tabular beds, white to brown in color, that display calcic and vertic pedofeatures. Internally, these palaeosols exhibit variations in the arrangement of soil aggregates ranging from massive to subangular blocky structure. The most conspicuous pedofeature is the presence of calcium carbonate, which can be in the form of individual nodules or as pervasively cemented calcretes.

4.2.1. Vertisols

4.2.1.1. Description. Vertisols are abundant in the lower and middle PSAA. They are developed in silts and silty sands assigned to AE 5 bodies. Their lateral extent exceeds hundreds of meters, but they are commonly cut by channel-fill deposits of AE 1 and 2. Some of the diagnostic features are (Table 1): slickensides, pseudo-anticlines, desiccation cracks (Fig. 4h), a prismatic structure (Fig. 5a) and occasionally carbonate nodules. Bioturbation in these palaeosols is intense: the trace fossils are mainly *T. serpentinum* and *Castrichnus incolumis* (Beilinson and Taglioretti, 2013). Micromorphological studies of these palaeosols also identified Fe-nodules (0.2–0.5 mm diameter), clay coatings and hypocoatings and a porostriated to granostriated b-fabric (Fig. 5b,c). Clay mineralogy of the <4 μm fraction indicated the presence, in decreasing order of abundance, of illite (I), smectite (Sm), kaolinite (K), chlorite (Ch) and mixed-layer illite/smectite (I/S) (Table 1).

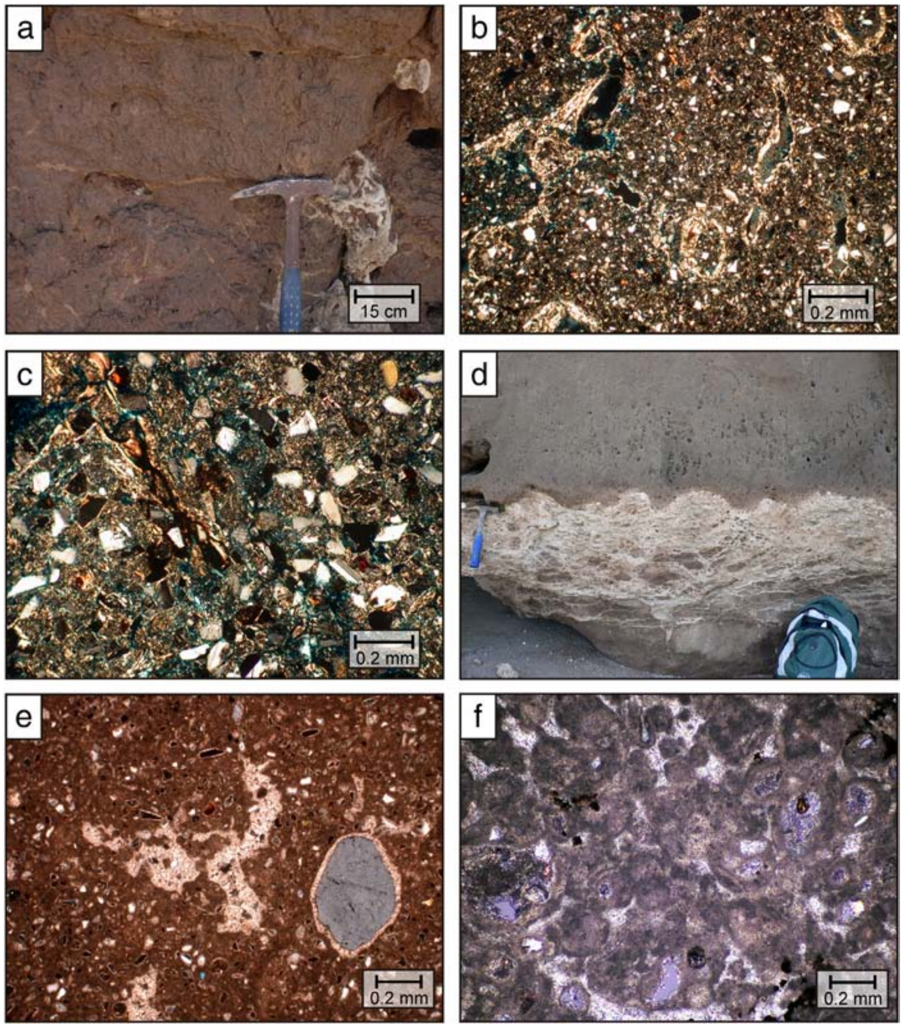

Fig. 5. Pedofeatures of the Punta San Andrés Alloformation palaeosols. a) Slickensides, prismatic structure and carbonate nodules in a Vertisol; b and c) Vertisols: microphotography of clay coatings and hypo-coatings and a porostriated to granostriated b-fabric; d) Calcisol: upper contact is represented by dissolution features; e) alpha microfabrics in a Calcisol: homogeneous calcite-rich groundmass with calcitic crystallitic b-fabric and floating detrital grains; f) beta microfabrics in a Calcisol: pisoliths, coated grains, disseminated organic matter and microstructures.

4.2.1.2. Classification and palaeoenvironment. These palaeosols were classified as Vertisols since their most prominent features are related to processes of pedoturbation by shrinking and swelling of expandable clays.

Palaeosols usually contain several palaeoenvironmental indicators. In the case of the studied Vertisols, the relative high concentration of smectite (Table 1) is interpreted to reflect low-lying and poorly drained conditions while the occurrence of mixed-layer illite/smectite points to a strong seasonality (Thiry, 2000). The presence of earthworm trace fossils suggests relatively high humidity (Verde et al., 2007; Beilinson and Taglioretti, 2013) although seasonal precipitation (Verde et al., 2007). The appearance of Fe/Mn mottles was also related to considerable soil moisture and poor soil drainage.

4.2.2. Calcisols

4.2.2.1. Description. Calcisols are conspicuously represented in the PSAA and are composed of sub-horizontal tabular units with a lateral extent of several kilometers. Diagnostic features include multiple horizons of nodular, laminar and massive morphology. Typically, the upper contact is represented by dissolution features and an erosional surface (Fig. 5d). The lower contact tends to be gradational. Micromorphological features include a homogeneous calcite-rich groundmass with calcitic crystallitic b-fabric (*sensu* Stoops et al., 2010) with widely scattered, floating detrital grains (alpha microfabrics) (Fig. 5e). Different types of beta microfabrics were also identified: laminar crusts, pisoliths, coated grains, disseminated organic matter and microstructures indicative of microbial influence on calcite precipitation (*i.e.*, alveolar-septal structure) (Fig. 5f). Scarce trace fossils such as *T. serpentinum* (Beilinson, 2011) were found in these horizons.

4.2.2.2. Classification and palaeoenvironment. The development of Calcisols is related to mean annual precipitation below 1000 mm and strong evaporation. This was suggested by the presence of halite and barite crystals in upper horizons. The PSAA Calcisols had good drainage conditions, as there were no possibility of ponding or soil saturation. A high concentration of kaolinite (Table 1) indicates relatively well-drained soils (Sheldon and Tabor, 2009), while the presence of pedogenic carbonates points to a non-humid climate (Retallack and Alonzo-Zarza, 1998).

4.2.3. Protosols

4.2.3.1. Description. Protosols are poorly represented and are developed on medium to fine sands and silty sands of AE 4. These sub-horizontal, tabular units are hundreds of meters of lateral extent and tend to be interrupted by channel-fill deposits of AE 1 and 2. Diagnostic features

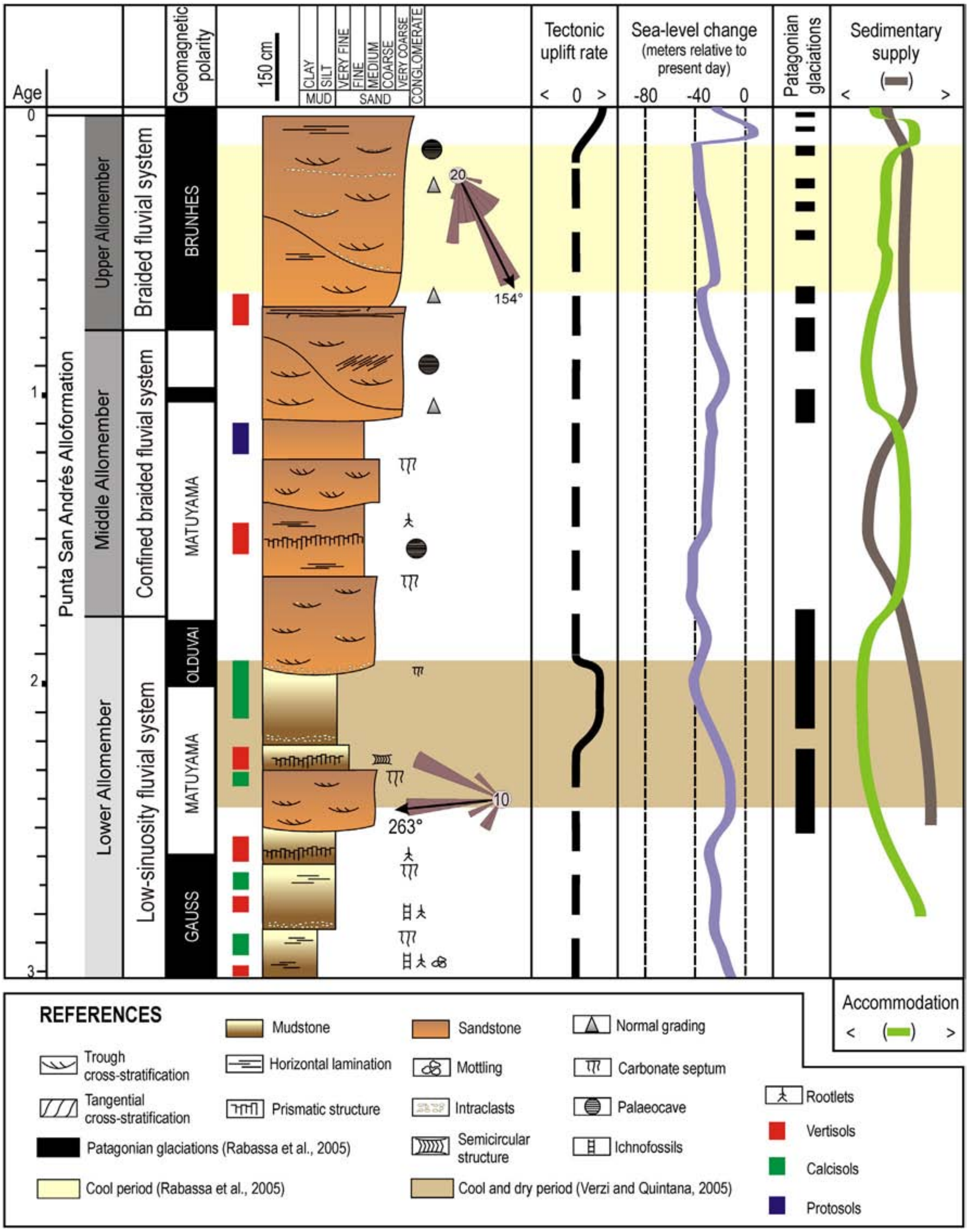

Fig. 6. Integrated stratigraphic column of the Punta San Andrés Alloformation.

of Protosols include carbonate nodules (5 to 10 cm diameter) and poor horizonation. Bioturbation of these palaeosols is due to *T. serpentinum* and *B. coronus* (Beilinson and Taglioretti, 2013). Petrographic analysis showed very few indicators of pedogenic activity such as poorly developed b-fabric and evidence of roots.

4.2.3.2. Classification and palaeoenvironment. These palaeosols are classified as Protosols because they display inmature argillans, carbonate or *in situ* mineral alteration. The Protosols show variable clay mineral content, with extremes rich in smectite and others rich in illite or kaolinite. This, together with the low degree of palaeosol development, limits palaeoenvironmental interpretations.

4.3. Depositional styles

The PSAA deposits were previously interpreted by Zárate (1989) and Beilinson (2009, 2011, 2012) as a fluvial/alluvial succession. The new observations presented here shows the detailed nature and evolution of fluvial styles within this unit. Interpretation is based on the presence of coarse-grained in fill of the sand bodies; their ribbon geometries;

distinct palaeocurrent directions in single channels; internal structure and sorting; and different types of palaeosols. Three fluvial styles are recognized.

4.3.1. Low-sinuosity fluvial system

The lower allomember of the PSAA (Fig. 6) is characterized by floodplain architectural elements (AE 4 and 5) in which four Calcisols and four Vertisols were identified (Fig. 6). Upwards, each Calcisol shows a more mature profile than the previous one. The palaeosol at the top of the lower allomember is the most mature, with tabular geometry hundreds of meters wide and 2 m thick. It displays Stage V and VI morphologies (Machette, 1985) and is the only one where halite and barite crystals are found. Vertisols show the same maturity in all of their profiles. For Calcisols and Vertisols the high illite/kaolinite ratio (Table 1) suggests arid and cold conditions (Suresh et al., 2004). The sheet bodies of the AE 4 are interpreted as crevasse splay complexes formed by repeated channel avulsion (Aslan and Blum, 1999; Blum and Aslan, 2006), related to high accommodation and sediment supply (Aslan and Blum, 1999). Secondary effluents and/or crevasse-channels (AE 2) are found adjacent to channel deposits (AE 1).

4.3.2. Confined braided fluvial system

The middle allomember (Fig. 6) is characterized by proximal floodplain deposits (AE 3, 4 and 5) and a higher proportion of channel-fill deposits (AE 1 and 2) than the lower allomember. Palaeosols found in this section are as Vertisols and Protosols. The complex internal arrangement of sands and pebbly sands within the AE 1 resulted from avulsion of smaller channels within the major trunk channel belt and by lateral or downstream migration of bars (Bentham et al., 1993) (Fig. 3g). These suggests braided rivers. In the middle section of the PSAA, AE 1 and 2 deposits are encased in floodplain deposits. For these atypical braided fluvial systems, where large volumes of fine-grained material is preserved and surrounds individual braided channels, Bentham et al. (1993) have proposed the confined braided fluvial system facies model.

4.3.3. Unconfined braided fluvial system

Multistory fluvial channels (AE 1) dominate the upper allomember (Fig. 6) and have tabular geometry. Planar and trough cross-stratified sands within basal scours are interpreted to reflect the infilling of channels by migration of dune forms. The upward termination of the channel-fill shows low-stage re-working of larger bedforms. A classical braided fluvial system was proposed for this succession (Beilinson, 2011).

5. Sequence stratigraphy

For the Punta San Andrés Alloformation, the absence of marine deposits and problems in correlating across the Buenos Aires region makes it difficult to use classical sequence stratigraphical terminology. Dahle et al. (1997) provide a solution for this problem by introducing the terminology of high- and low-accommodation system tracts. These system tracts were specifically designed to describe fluvial deposits that accumulated free of marine or lacustrine influence or whose contemporary coastline cannot be correlated clearly. The high- and low-accommodation system tracts are defined mainly on the basis of architectural elements present in the succession, also taking into account the relative proportion of channel deposits and floodplain deposits. These constitute assumptions of the changes in fluvial accommodation in time (Dahle et al., 1997; Catuneanu, 2006) (Table 4). However, changes in sediment supply can also lead to similar variations in accumulation conditions (Miall, 2002). Taking these into account, the system tracts described here refer to periods in which there was an increase or decrease in the rate of generation of accommodation. They refer to tendencies in accommodation and sedimentation with no implications for relative sea level.

Table 4
Defining features of the low- and high-accommodation system tracts.
Modified from Catuneanu (2006).

	Low-accommodation system tract	High-accommodation system tract
Depositional trend	Early progradational	Aggradational
Depositional energy	Early increase, then decline	Decline through time
Grading	Coarsening-upward at base	Fining-upward
Grain size	Coarser	Finer
Geometry	Irregular, discontinuous	Tabular or wedge-shaped
Sand:mud ratio	High	Low
Architecture	Amalgamated cannel fills	Isolated ribbon sandstones
Floodplain facies	Sparse	Abundant
Thickness	Tends to be thinner	Tends to be thicker
Coal seams	Minor or absent	Well developed
Paleosols	Well developed	Poorly developed

5.1. General sequence stratigraphic framework

Parker et al. (2008) proposed a general sequence stratigraphic framework for the late Cenozoic deposits of the south-eastern Buenos Aires province. Their work was based on seismostratigraphic sequences from the Bonaerenian continental platform that were correlated to lithostratigraphic units in the continental coastal area (Fig. 7). For these authors, each seismostratigraphic sequence (or depositional sequence; DS) represents a transgressive–regressive cycle that is bounded at its base and top by discontinuities identified as terminations of seismic reflectors. These terminations were interpreted as the result of either subaerial erosion during lowstands or subaqueous erosion during transgressions. Even though the hierarchy of the sequences was not defined by Parker et al. (2008), the proposed glacio-eustatic forcing of 0.7 to 1.2 Ma might be related to third- or fourth-order sequences established by Vail et al. (1991) and Posamentier and Allen (1999).

5.2. Proposed sequence stratigraphic model for the Punta San Andrés Alloformation

Compatible with Parker et al. (2008), the general sequence stratigraphic framework of the Punta San Andrés Alloformation is shown (Fig. 8). Two high-accommodation system tracts and two low-accommodation system tracts were identified based on internal stratigraphic surfaces and bounding surfaces (Figs. 8, 9).

5.2.1. High-accommodation system tract 0 (HAST 0)

The base of the PSAA was located south of the Las Brusquitas Creek (Fig. 1b) by Zárate (1989), but the nature of this surface could not be assessed in the present study because it does not crop. Nevertheless, the architecture of the low-sinuosity fluvial system at the base of the Punta San Andrés Alloformation, together with its spatial distribution and the relationships with underlying units (Playa Los Lobos and Punta Martínez de Hoz alloformations) made it possible to reconstruct relative accommodation and sedimentation rate conditions.

The Playa Los Lobos and Punta Martínez de Hoz alloformations are characterized by reddish fine-grained sediments with the development of hydromorphic palaeosols (Zárate, 1989). Channel-fill deposits are nearly absent. Where present, they show a ribbon-like geometry with $W/D < 15$ and a slightly asymmetric silt infill. The transition to the low-sinuosity fluvial system of the PSAA reflects a shift to coarser-grained units and a higher proportion of channel-fill deposits.

During normal regression that accompanies a high-accommodation system tract (Posamentier and Allen, 1999), coastal areas show a decrease in the rate of generation of accommodation. This fact is directly related to a decrease in topographic gradient, which in turn leads to a decrease in fluvial energy flux and to fining-upward successions. Although this applies to the early stages of high-accommodation system

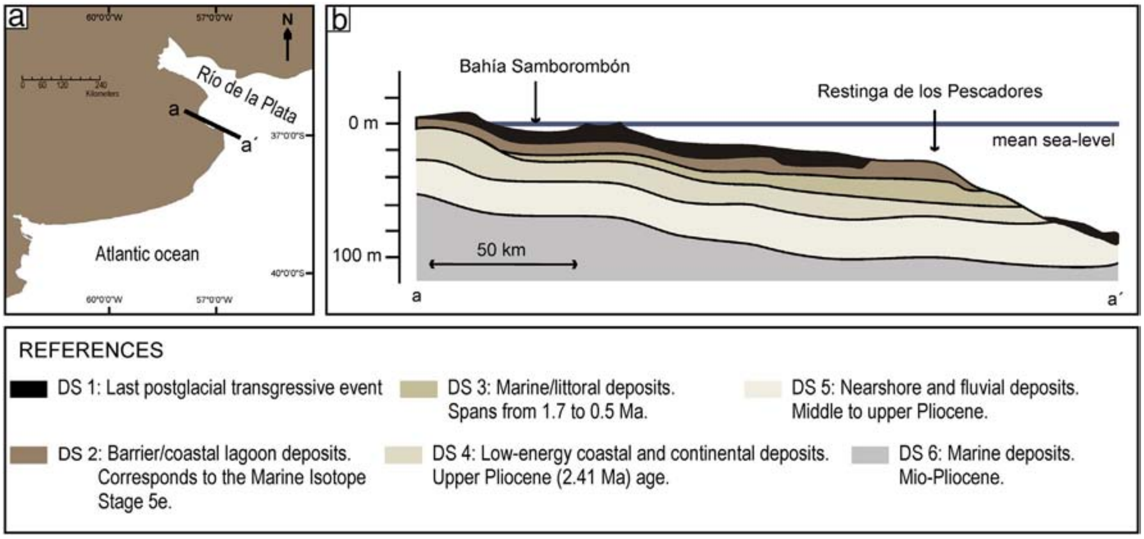

Fig. 7. Seismostratigraphic chart of Bonaerenian late Cenozoic units. a) Location map of the seismic transect; b) note the progradational distribution of depositional sequences (DS). Modified from Parker et al. (2008).

tracts, the final stages may be characterized by channel systems that are interconnected and amalgamated due to the lack of fluvial accommodation once the relative sea-level rise rate decreases and reaches zero (Aitken and Flint, 1994; Catuneanu, 2006). Therefore, this system tract may be divided into a lower section, with isolated channel fills surrounded by fine-grained, strongly aggradational floodplain deposits, and an upper section with a higher degree of channel amalgamation. Consequently, the ratio between floodplain and channel-fill architectural elements also tends to be higher (Catuneanu, 2006).

In the deposits of the PSAA, different avulsion styles have been identified. In low-sinuosity system channels are narrow (<20 m wide), lack levees and do not form alluvial belts. The channel-fill facies are also surrounded by massive floodplain deposits with palaeosols (Fig. 10). These characteristics suggest that the dominant avulsion style was channel diversion towards a low-lying plain, with no reoccupation of former channels. The low-sinuosity fluvial system of the PSAA is therefore interpreted as a high-accommodation system tract (Fig. 8) with minor oscillations that might be attributed to climatic or autocylic processes. This interpretation coincides with the sea-level curves for the Pliocene and Pleistocene (Fig. 6).

5.2.2. Sequence boundary 1 (SB 1)

The top of the low-sinuosity system of the PSAA is an irregular, highly erosional surface that can be traced for nearly 30 km. This surface clearly separates a very mature Clacisol from AE1 and 2 deposits of the overlying LAST 1.

5.2.3. Low-accommodation system tract 1 (LAST 1)

The LAST 1 overlies SB1 and is characterized by coarse-grained deposits that display trough and planar cross-bedding and are interpreted as channel-fill deposits (AE 1 and AE 2 architectural elements; Fig. 9a–c) that locally incise HAST 0 (Fig. 9a–b). The AE 1 deposits are channel-fill deposits that show lateral but no vertical amalgamation.

The architectural elements preserved in LAST 1 represent increased accommodation after development of a subaerial unconformity (Legarreta et al., 1993). Two stages can be recognized in the low-accommodation system tract (Table 2). The lower part shows low sediment accumulation due to limited accommodation. This results in preservation of basal deposits as conglomerates (*i.e.*, channel lags) and as basal segments of channel bars (Fig. 9). A shift to upper low-accommodation system tract indicates an increase in accommodation space in the fluvial reach. Here, infilling of channels that were active during the lower low-accommodation system tracts occur. The wings identified in several of the AE 1 sand bodies might be interpreted as the result of this process.

5.2.4. Maximum regression surface (MRS)

The top of LAST 1 deposits is represented by a laminated to massive non-pedogenic carbonate level, 7 to 10 cm thick, that overlies both floodplain deposits with Calcisol development of HAST 0, and channel-fill deposits of LAST 1, causing the overlapping of the MRS onto SB 1 (Fig. 9a,d).

In fluvial deposits, identification of a maximum regression surface may not always be straight forward. Although it coincides with a sharp decrease in fluvial energy, which usually translates into a change from amalgamated braided channels towards meandering systems (Catuneanu, 2006), this change might be gradual and therefore difficult to identify. In the PSAA, the laminated carbonate level is interpreted as a maximum regression surface. It indicates a change to conditions in which the rate of accommodation creation equals and eventually exceeds the rate of sediment supply.

5.2.5. High-accommodation system tract 1 (HAST 1)

The development of a confined braided fluvial system on top of the maximum regression surface suggests new accumulation conditions in the depositional basin with an increase in accommodation creation. A high rate of sediment supply is inferred (Figs. 6, 8), in which the fluvial channel infill was encased within floodplain sediments (Fig. 9c).

Unlike HAST 0, even though this system tract developed during high relative base-level, it represents lower accommodation conditions, possibly due to progradation of the basin evidenced by increased grain size. For the confined braided fluvial system of HAST 1 (Fig. 6), most of the channel belts show laterally and vertically amalgamated macroforms. Macroform amalgamation and, on a larger scale, channel-belt amalgamation represent autocyclic migration and displacement of the main and secondary channels by avulsion (Miall, 2006; Nichols and Fisher, 2007). The braided system is thus related to avulsion by reoccupation of previous channels, with the reworking of older deposits (Aslan and Blum, 1999; Blum and Aslan, 2006).

5.2.6. Sequence boundary 2 (SB 2)

The sequence boundary at the top of the confined braided system is erosive and irregular (Fig. 9d). The development of the amalgamated braided channels overlying this surface (Fig. 6) marks an abrupt change

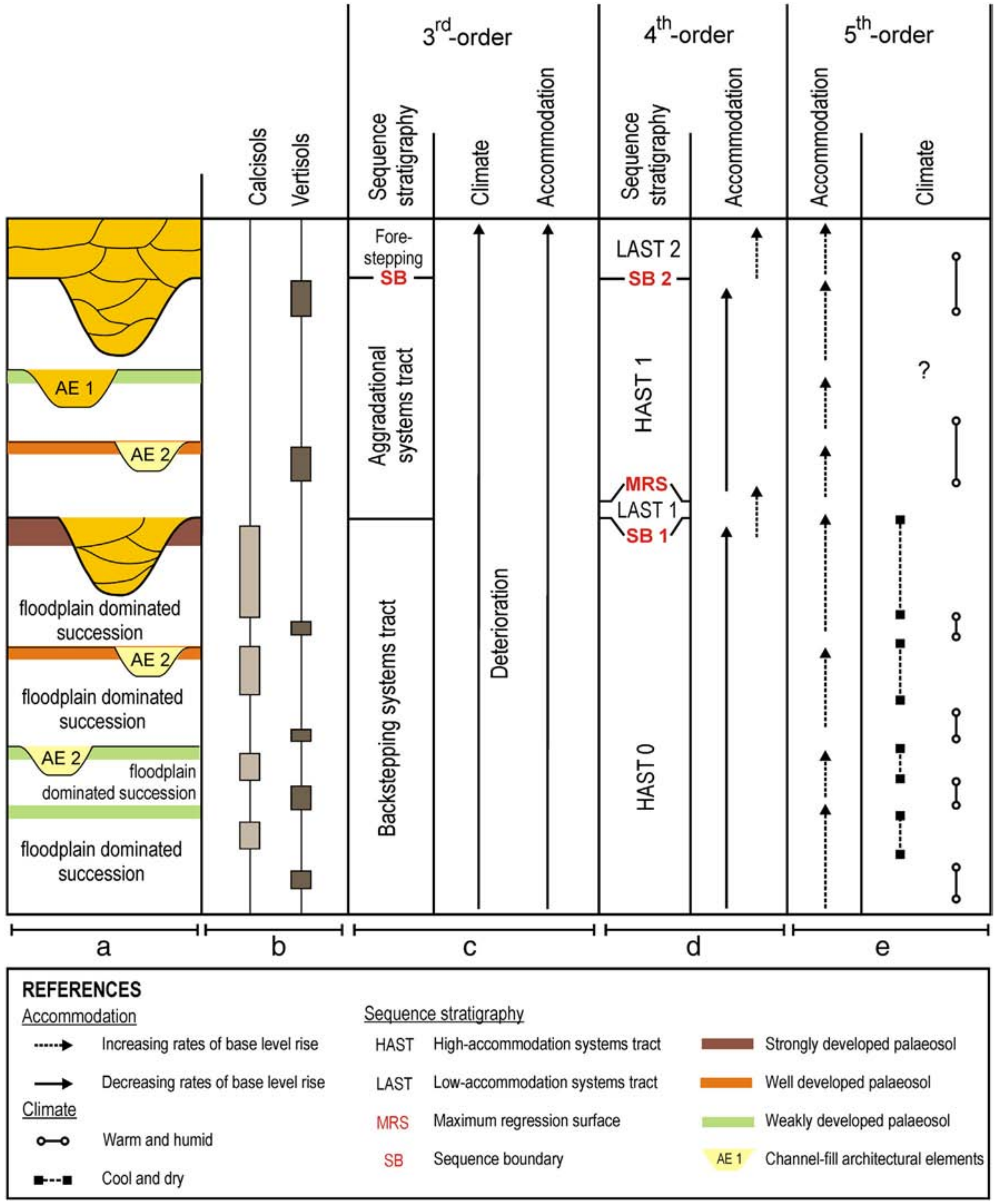

Fig. 8. Conceptual diagram summarizing the different hierarchies identified in the Punta San Andrés Alloformation. a) Stratigraphic succession; b) vertical distribution and relative abundance of paleosols; c) 3rd-order cycles with nomenclature. Trends in climate towards more arid and cool conditions (Ravelo et al., 2004) and decreasing rate of creation of accommodation space; d) 4th-order cycles with bounding surfaces and variations in accommodation; e) 5th-order cycles with alluvial and high-frequency climatic cycles. c, after Legarreta et al. (1993).

in dominant grain size and facies. Sea-level fall below the continental shelf edge (Violante, pers. comm.) related to Patagonian glaciations may have caused an increase in topographic gradient of fluvial channels and consequent increase in transport energy. SB 2 is considered to be a diachronic surface influenced by the glacial events which predominated during the upper Ensenadian and Bonaerenian.

5.2.7. Low-accommodation system tract 2 (LAST 2)

The remaining low-accommodation system tract comprises the upper section of the PSAA and shows a braided fluvial system with deep unconfined channels. LAST 2 is characterized by pebbly, very coarse to medium sands that display sets of trough and planar cross-bedding. When compared to LAST 1 deposits, LAST 2 shows more complex channel fill. In LAST 1, they are multilateral channels, locally incised in HAST 0, whereas LAST 2 deposits have a basal erosion surface with up to 5 m of relief and internally comprise 3 to 4 laterally shifted, vertically stacked stories. They are incised into HAST 1 deposits and locally even erode HAST 0 and LAST 1 deposits. LAST 2 represents the up-stream end of the fluvial system (Tandilia Range; Fig. 1a), the generation of accommodation space and higher discharge and transport capacity.

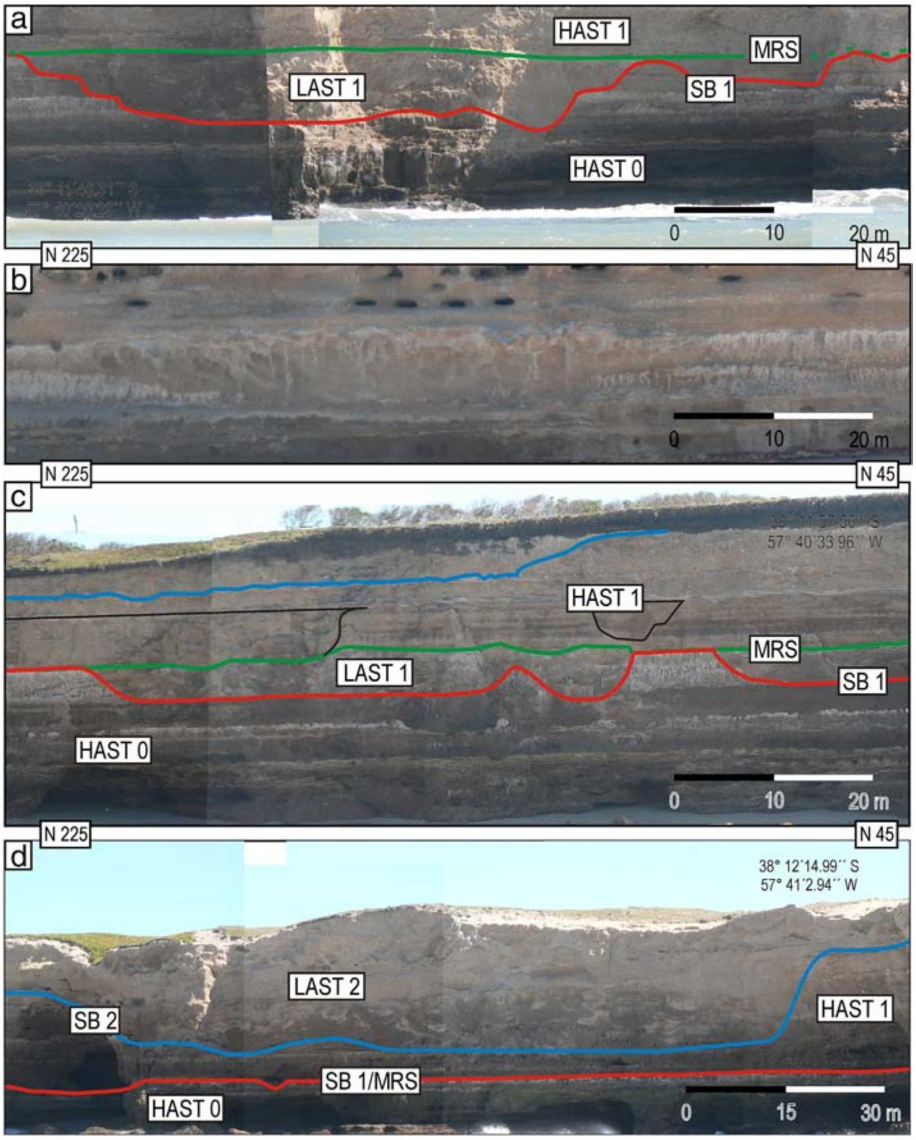

Fig. 9. Interpreted photomosaics showing: a, b) different system tracts and sequence boundaries (SB 1 and 2); c) LAST 1 represented by amalgamated channel fills above the maximum regressive surface (MRS); d) laminated to massive carbonate level overlying floodplain (HAST 0) and channel-fill deposits (LAST 1).

6. Discussion

During accumulation of the Punta San Andrés Alloformation, the combination of the glacio-eustasy and climate directly conditioned the balance between accommodation and sediment supply (Fig. 6). However, analysis of architectural elements, their vertical stacking pattern, palaeosols and clay minerals enables the identification of fifth-, fourth- and third-order sequences (Fig. 8). Here, fifth-order sequences are defined by means of palaeosols, fourth-order sequences are identified by means of high- and low-accommodation system tracts, and the only third-order sequence comprises the entire Punta San Andrés Alloformation (Fig. 8).

The mountains source areas provided abundant material to the basin. The climate, though seasonal, with its gradual change towards cold and dry conditions in the upper Pleistocene, greatly conditioned the development of palaeosols.

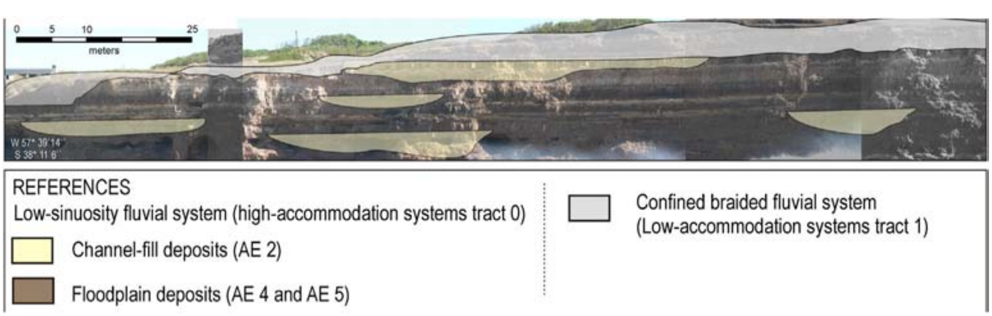

Fig. 10. Interpreted photomosaic of low-sinuosity fluvial system (high-accommodation system tract 0).

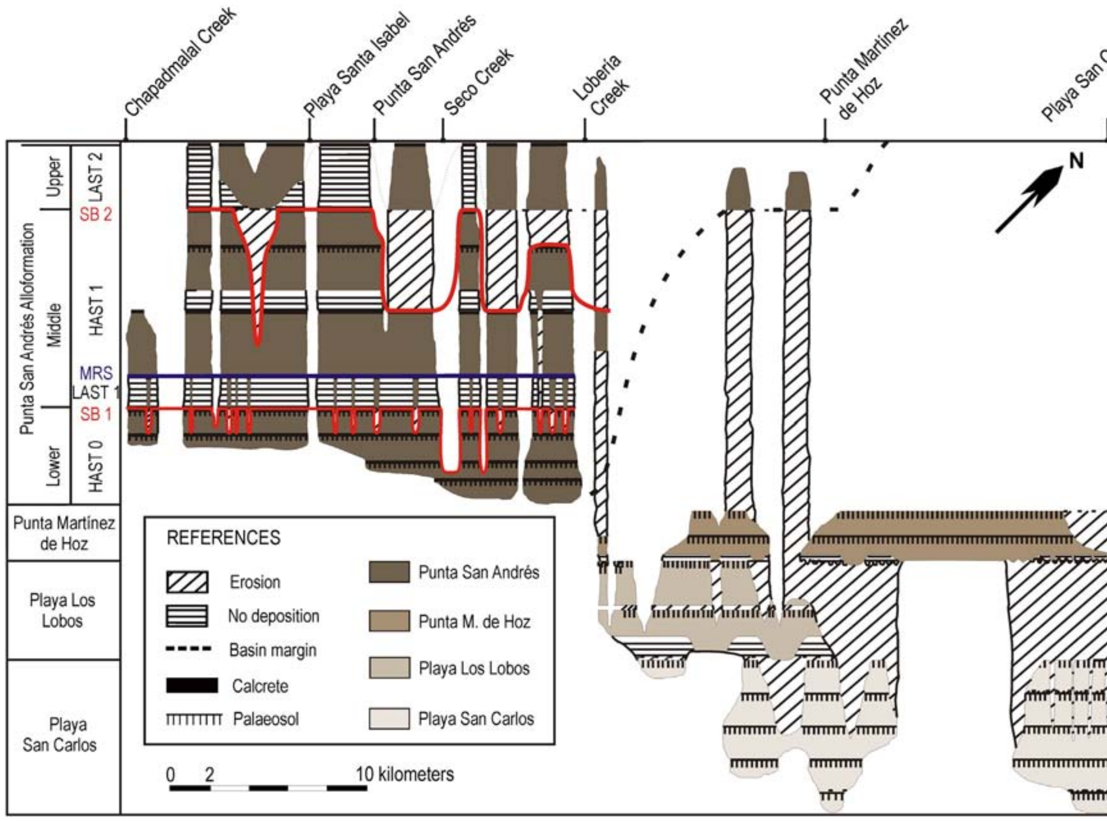

Fig. 11. Lithostratigraphic chart of the Cenozoic deposits in the study area. Notice the south-western displacement of the units between Punta Martínez de Hoz and Punta San Andrés alloformations.

During deposition of HAST 0, the climate was characterized by high-frequency cyclic variations that led to the development of intercalated Vertisols and Calcisols in floodplain deposits. These may be regarded as cycles of fluvial aggradation (Atchley et al., 2004) or of fifth-order, in which fluctuations in base level — caused by climate — generated cycles in accommodation and sediment supply (Figs. 6, 8). Based on palaeosols alone, a general tendency towards higher aridity can be deduced, suggested by the presence of halite and barite crystals in upper stratigraphic horizons.

It is useful to establish a correlation between different scales of climate variation and glacial events (Fig. 6). Rabassa et al. (2005) identified a glaciation between 2.43 and 2.25 Ma (Sanandresian stage), which may correspond to the youngest strata of HAST 0 containing a highly developed Calcisol with evaporites. Therefore, it is proposed that glaciation caused a lowered water table at this time.

The fluvial system during HAST 0 adopted a low-sinuosity pattern as a consequence of high accommodation space. Towards the end of HAST 0, Patagonian glaciations triggered a decrease in local base level recorded in SB 1, with consequent rejuvenation of the fluvial system and incision of floodplain deposits (Figs. 6, 8).

The fact that outcrops of HAST 0 are found only in the Punta San Andrés, Playa Santa Isabel and Chapadmalal areas (Fig. 11) suggests that this was the lowest part of the basin or had the highest subsidence. As there is no evidence of syn-depositional faults, it suggests that it was topographically lower. This observation coincides with the basin geometry proposed by Zárate (1989) of a shallow basin with gently-sloped margins and its center near the Lobería Creek.

After LAST 1, deposition was no longer concentrated in the topographic lows and spreads across the wider basin (Fig. 11). During this period, climate was a fundamental control on accommodation space due to its influence on glacio-eustasy, favoring an increase in accommodation during HAST 1 and decrease during SB 2 (Figs. 6, 8). The decrease in sea level at the end of the Pleistocene caused the coastal depositional systems to prograde towards the basin. The deposits of HAST 1 are thicker, coarser and have a higher proportion of channel-fill deposits than HAST 0.

After SB 2, renewed deposition was connected to the development of large braided channels which amalgamated laterally and vertically, reflecting low accommodation conditions (LAST 2). This may suggest that, although glacial periods have an increased sediment supply, it is at the beginning of interglacials when the largest sediment influx to the basin occurs (Waters and Haynes, 2001). As a consequence, a significant increase in fluvial sediment transport can be assumed, building the middle and upper allomembers of the Punta San Andrés Alloformation. LAST 2 may have enhanced the low-accommodation by means of high sediment supply (Fig. 6).

The Punta San Andrés Alloformation may also be set within a context of third-order sequences, spanning the 3.1 Ma that its deposits represent (Fig. 8). The fourth-order HAST 0 may therefore be interpreted as a third-order retrogradational system tract (or 'backstepping system tract' *sensu* Legarreta et al., 1993) in which rapid sea-level rise creates accommodation at a higher rate than sediment is supplied, favoring the development of large floodplains and channel-fill deposits. The fourth-order sequence between SB 1 and SB 2 would correspond to a third-order aggradational system tract (*sensu* Legarreta et al., 1993; Fig. 8), in which the aggradational to progradational arrangement of the depositional elements indicates a decrease in accommodation space associated with eustatic sea level fall during the lower Pleistocene. The fourth-order SB 2 coincides with the third-order sequence boundary. Deposits of LAST 2 may be assigned to a third-order progradational system tract (or 'forestepping system tract' *sensu* Legarreta et al., 1993; Fig. 8), in which deposition within incised valleys predominates and deposition in the floodplains is greatly restricted (Figs. 8, 9d).

Therefore, the development of the third-order sequence associated with the Punta San Andrés Alloformation may be interpreted as the progradation of continental depositional systems, characterized by a braided system in the proximal areas, and a low-sinuosity, single-channel system in the distal areas, defined by a high rate of sediment supply and discharge peaks which periodically flooded the plains and generated high aggradation rates during the late Pliocene and lower Pleistocene.

7. Conclusions

(1) The Punta San Andrés Alloformation is characterized by a fluvio-alluvial succession which displays channel-fill and floodplain deposits. The former show an upward trend from single to multi-story channels. Floodplain facies tend to decrease upwards with concomitant development of Calcisols and Vertisols.

(2) During accumulation of the Punta San Andrés Alloformation, the combination of glacio-eustasy and climate directly controlled the balance between generation of accommodation space and sediment supply. The clay content of palaeosols and their pedo-features indicate climatic deterioration with strong seasonality. Analysis of the architectural elements indicates a general reduction in accommodation space.

(3) A high-resolution sequence stratigraphic model shows two high-accommodation system tracts and two low-accommodation system tracts.

(4) Both sequence boundaries are accompanied by development of incised valleys linked to relative sea-level fall.

(5) Fifth-, fourth- and third-order hierarchies were identified and interpreted in terms of accommodation and climate change. Alongside the proposed general stratigraphic model they could be applied to other sequences that were deposited during periods of climatic deterioration.

Acknowledgments

The authors thank the logistical support for the field work provided by the Centro de Investigaciones Geológicas. Valuable reviews by J. Knight and two anonymous reviewers greatly improved the final manuscript. This study was funded by the CONICET doctoral and post-doctoral grants, awarded to E. Beilinson.

References

Abdul Aziz, H., Sanz-Rubio, E., Calvo, J.P., Hilgen, F.J., Krijgsman, W., 2003. Palaeoenvironmental reconstruction of a middle Miocene alluvial fan to cyclic shallow lacustrine depositional system in the Calatayud Basin (NE Spain). Sedimentology 50, 211–236.

Aitken, J.F., Flint, S.S., 1994. High-frequency sequences and the nature of incised-valley fills in fluvial systems of the Breathitt Group (Pennsylvanian), Appalachian foreland basin, eastern Kentucky. In: Dalrymple, R.W., Boyd, R., Zaitlin, B.A. (Eds.), Incised Valley Systems: Origin and Sedimentary Sequences. SEPM Special Publication, 51, pp. 353–368.

Aslan, A., Blum, M.D., 1999. Contrasting styles of Holocene avulsion, Texas Gulf coastal plain, USA. In: Smith, N.D., Rogers, J. (Eds.), Fluvial Sedimentology VI. IAS Special Publication, 28, pp. 193–209.

Atchley, S.C., Nordt, L.C., Dworkin, S.I., 2004. Eustatic control on alluvial sequences stratigraphy: a possible example from the Cretaceous–Tertiary transition of the Tornillo Basin, Big Bend National Park, west Texas, U.S.A. J. Sediment. Res. 74, 391–404.

Beilinson, E., 2009. Análisis de facies y paleoambiental de alta resolución de la Aloformación Punta San Andrés (Plio-Pleistoceno), provincia de Buenos Aires, Argentina. Lat. Am. J. Sedimentol. Basin Anal. 16 (1), 57–74.

Beilinson, E., 2011. Estratigrafía secuencial de alta resolución y análisis arquitectural de cuerpos en sistemas fluviales de la Aloformación Punta San Andrés (Plio-Pleistoceno), Barrancas de Miramar a Mar del Plata. (Ph. D. thesis) National University of La Plata, Argentina.

Beilinson, E., 2012. Evolución de la arquitectura fluvial en sucesiones del Plioceno-Pleistoceno del centro-este de Argentina (Aloformación Punta San Andrés). Rev. Asoc. Geol. Argent. 69 (3), 578–595.

Beilinson, E., Taglioretti, M.L., 2013. Análisis icnológico y paleoambiental de la Aloformación Punta San Andrés (Plio-Pleistoceno), provincia de Buenos Aires, Argentina. Ameghiniana 50, 153–165.

Bentham, P.A., Talling, P.J., Burkank, D.W., 1993. Braided stream and floodplain deposition in a rapidly aggrading basin: the Escanilla formation, Spanish Pyrenees. In: Best, J.L., Bristow, C.S. (Eds.), Braided Rivers. Geological Society Special Publication, 75, pp. 177–194.

Biscaye, P., 1965. Mineralogy and sedimentation of recent deep-sea clay in the Atlantic Ocean and adjacent seas and oceans. Geol. Soc. Am. Bull. 76, 803–832.

Blum, M.D., Aslan, A., 2006. Signatures of climate *vs.* sea-level change within incised valley-fill successions: Quaternary examples from the Texas Gulf Coast. Sediment. Geol. 190, 177–211.

Bullock, P., Fedoroff, N., Jongerius, A., Stoops, G., Tursina, T., 1985. Handbook for Soil Thin-Section Description. Waine Res. Publishing, Wolverhampton, UK (152 pp.).

Catuneanu, O., 2006. Principles of Sequence Stratigraphy. Elsevier, United Kingdom (387 pp.).

Cavallotto, J.L., Violante, R., 2005. Geología y geomorfología del Río de la Plata. In: de Barrio, R.E., Caballé, M.F., Llambías, E. (Eds.), Geología y recursos minerales de la Provincia de Buenos Aires. Relatorio del 16° Congreso Geológico Argentino, La Plata, pp. 237–254.

Chappell, J., Shackleton, N.J., 1986. Oxygen isotopes and sea level. Nature 324, 137–140.

Cione, A.L., Tonni, E.P., 1995. Chronostratigraphy and land mammal ages in the Cenozoic of southern South America: principles, practices and the Uquian problem. J. Palaeontol. 69, 135–159.

Cione, A.L., Tonni, E.P., 1999. Biostratigraphy and chronological scale of uppermost Cenozoic in the Pampean Area, Argentina. Quat. S. Am. Arct. Penins. 12, 23–51.

Cione, A.L., Tonni, E.P., 2005. Bioestratigrafía basada en mamíferos del Cenozoico superior de la provincia de Buenos Aires, Argentina. In: de Barrio, R.E., Caballé, M.F., Llambías, E. (Eds.), Geología y recursos minerales de la Provincia de Buenos Aires. Relatorio del 16° Congreso Geológico Argentino, La Plata, pp. 183–200.

Clapperton, C., 1993. Quaternary Geology and Geomorphology of South America. Elsevier Publishers, United Kingdom (779 pp.).

Clemente, P., Pérez-Arlucea, M., 1993. Depositional architecture of the Cuerda del Pozo Formation, Lower Cretaceous of the extensional Cameros Basin, North-Central Spain. J. Sediment. Petrol. 63 (3), 437–452.

Dahle, K., Flesja, K., Talbot, M.R., Dreyer, T., 1997. Correlation of fluvial deposits by the use of Sm–Nd isotope analysis and mapping of sedimentary architecture in the Escanilla Formation (Ainsa Basin, Spain) and the Statfjord Formation (Norwegian North Sea). Abstracts, Sixth International Conference on Fluvial Sedimentology, Cape Town, South Africa, p. 46.

Folguera, A., Zárate, M.A., 2011. Neogene sedimentation in the Argentine foreland between 34° 30′S and 41° S and its relations to the Andes evolution. In: Salfity, J., Marquillas, R. (Eds.), Cenozoic Geology of the Central Andes of Argentina. SCS Publishers, Argentina, pp. 123–134.

García-Gil, S., 1993. The fluvial architecture of the upper Buntsandstein in the Iberian Basin, central Spain. Sedimentology 40, 125–143.

Ghosh, P., Sarkar, S., Maulik, P., 2006. Sedimentology of a muddy alluvial deposit: Triassic Denwa Formation, India. Sediment. Geol. 191, 3–36.

Gibling, M.R., 2006. Width and thickness of fluvial channel bodies and valley fills in the geological record: a literature compilation and classification. J. Sediment. Res. 76, 731–770.

Imbrie, J.J., Hays, J.D., Martinson, D.G., McIntyre, A., Mix, A.C., Moreley, J.J., Pisias, N.G., Prell, W.L., Shackleton, N.J., 1984. The orbital theory of Pleistocene climate: support from a revised chronology of the marine $\delta^{18}O$ record. In: Berger, A.L., Imbrie, J., Hays, J., Kukla, G., Saltzman, B. (Eds.), Milankovitch and Climate—Part 1. Reidel Publishing, pp. 269–306.

Legarreta, L., Uliana, M.A., Larotonda, C.A., Meconi, G.R., 1993. Approaches to non-marine sequence stratigraphy — theoretical models and examples from Argentine basins. In: Eschard, R., Doliez, B. (Eds.), Subsurface Reservoir Characterization from Outcrop Observations. Technip Editions, Paris, pp. 125–145.

Machette, M.N., 1985. Calcic soils of south-western United States. In: Weide, D.J. (Ed.), Soil and Quaternary geology of the south-western United States. Geological Society of America Special Paper, 203, pp. 1–21.

Mack, G.H., James, W.C., Monger, H.C., 1993. Classification of paleosols. Geological Society of America. Bulletin 105, 129–136.

Marshall, L.G., 1985. Geochronology and land-mammal biochronology of the Transamerican Faunal Interchange. In: Stehil, F.G., Webb, S.D. (Eds.), The Great American Biotic Interchange. Plenum Press, New York and London.

Miall, A.D., 1978. Fluvial sedimentology. Canadian Society of Petroleum Geologists Memoir, 5 (620 pp.).

Miall, A.D., 2002. Architecture and sequence stratigraphy of Pleistocene fluvial systems in the Malay Basin based on seismic time-slice analysis. AAPG Bulletin 86 (7), 1201–1216.

Miall, A.D., 2006. The geology of fluvial deposits. Sedimentary Facies, Basin Analysis and Petroleum Geology.Springer, Germany (582 pp.).

Moore, D., Reynolds, R., 1989. X-Ray Diffraction and the Identification and Analysis of Clay Minerals. Oxford University Press, Oxford (332 pp.).

Nichols, G.J., Fisher, J.A., 2007. Processes, facies and architecture of fluvial distributary system deposits. Sediment. Geol. 195, 75–90.

North, C.P., Davidson, S.K., 2012. Unconfined alluvial flow processes: recognition and interpretation of their deposits, and the significance for palaeogeographic reconstruction. Earth Sci. Rev. 111, 199–223.

Paredes, J.M., Foix, N., Colombo Piñol, F., Nillni, A., Allard, J.O., Marquillas, R.A., 2007. Volcanic and climatic controls on fluvial style in a high-energy system: the Lower Cretaceous Matasiete Formation, Golfo San Jorge basin, Argentina. Sediment. Geol. 202 (1–2), 96–123.

Parker, G., Violante, R., Paterlini, M., Costa, I., Marcolini, S., Cavallotto, J., 2008. Las secuencias depositacionales del Plioceno-Cuaternario de la plataforma submarina adyacente al litoral del este bonaerense. Lat. Am. J. Sedimentol. Basin Anal. 15 (2), 105–124.

Pedoja, K., Husson, L., Regard, V., Cobbold, P.R., Ostanciaux, E., Johnson, M.E., Kershaw, S., Saillard, M., Martinod, J., Furgerot, L., Weill, P., Delcaillau, B., 2011. Relative sea-level fall since the last interglacial stage: are coasts uplifting worldwide? Earth Sci. Rev. 108, 1–15.

Posamentier, H.W., Allen, G.P., 1999. Siliciclastic sequence stratigraphy — concepts and applications. SEPM Concepts in Sedimentology and Paleontology #7, Tulsa, USA. (210 p.).
Rabassa, J., Coronato, A., 2009. Glaciations in Patagonia and Tierra del Fuego during the Ensenadan Stage/Age (Early Pleistocene–earliest Middle Pleistocene). Quat. Int. 210, 18–36.
Rabassa, J., Coronato, A., Salemme, M., 2005. Chronology of the Late Cenozoic Patagonian glaciations and their correlation with biostratigraphic units of the Pampean region (Argentina). J. S. Am. Earth Sci. 20, 81–104.
Ravelo, A.C., Andreasen, D.H., Lyle, M., Lyle, A.O., Wara, M.W., 2004. Regional climate shifts caused by gradual global cooling in the Pliocene epoch. Nature 429, 263–267.
Retallack, G.J., Alonzo-Zarza, A.M., 1998. Middle Triassic paleosols and paleoclimate of Antarctica. J. Sediment. Res. 68, 169–184.
Schultz, P., Zárate, M., Hames, W., Camilión, C., King, J., 1998. A 3.3 Ma impact in Argentina and possible consequences. Science 282, 2061–2063.
Sheldon, N.D., Tabor, N.J., 2009. Quantitative paleoenvironmental and paleoclimatic reconstruction using paleosols. Earth Sci. Rev. 95, 1–52.
Smith, N.D., Pérez-Arlucea, M., 2008. Natural levee deposition during the 2005 flood of the Saskatchewan River. Geomorphology 101, 583–594.
Stoops, G., Marcelino, V., Mees, F., 2010. Interpretation of Micromorphological Features of Soils and Regolithis. Elsevier Publishing, The Netherlands (720 pp.).
Suresh, N., Ghosh, S., Kumar, R., Sangode, S., 2004. Clay-mineral distribution patterns in late Neogene fluvial sediments of the Subathu sub-basin, central sector of Himalayan foreland basin: implications for provenance and climate. Sediment. Geol. 163, 265–278.
Teruggi, M.E., Etchichury, M.C., Remiro, J.R., 1957. Estudio sedimentológico de los terrenos de las barrancas de la zona Mar del Plata – Miramar. Rev. Mus. Argent. Cienc. Nat. Bernardino Rivadavia 4 (2), 1–210.
Thiry, M., 2000. Paleoclimatic interpretation of clay minerals in marine deposits: an outlook from the continental origin. Earth Sci. Rev. 49, 201–221.
Turic, M.A., Nevistic, A.V., Rebay, G., 1996. Geología y Recursos Naturales de la Plataforma Continental. In: Ramos, V.A., Turic, M.A. (Eds.), Geología y Recursos Naturales de la Plataforma Continental Argentina. Relatorio XIII Congreso Geológico Argentino y III Congreso de Exploración de Hidrocarburos, Buenos Aires, pp. 405–423.
Vail, P.R., Audemard, F., Bowman, S.A., Eisner, P.N., Perez-Cruz, C., 1991. The stratigraphic signatures of tectonics, eustacy and sedimentology—an overview. In: Einsele, G., Ricken, W., Seilacher, A. (Eds.), Cycles and Events in Stratigraphy. Springer-Verlag, Berlin, pp. 617–659.
Verde, M., Ubilla, M., Jiménez, J.J., Genise, J.F., 2007. A new earthworm trace fossil from paleosols: aestivation chambers from the Late Pleistocene Sopas Formation of Uruguay. Palaeogeogr. Palaeoclimatol. Palaeoecol. 243, 339–347.
Waelbroeck, C., Labeyrie, L., Michel, E., Duplessy, J.C., McManus, J.F., Lambeck, K., Balbona, E., Labracherie, M., 2002. Sea-level and deep water temperature changes derived from benthic foraminifera isotopic records. Quat. Sci. Rev. 21, 295–305.
Waters, M.R., Haynes, C.V., 2001. Late Quaternary arroyo formation and climate change in the American Southwest. Geology 29, 399–402.
Williams, D.F., Thunnell, R.C., Tappa, E., Rio, D., Raffi, I., 1988. Chronology of the Pleistocene oxygen isotope record, 0–1.88 Ma before present. Palaeogeogr. Palaeoclimatol. Palaeoecol. 64, 221–240.
Zárate, M.A., 1989. Estratigrafía y geología de los acantilados marinos comprendidos entre Playa San Carlos y Arroyo Chapadmalal. (Ph. D. thesis) National University of La Plata, Argentina.
Zárate, M.A., 2005. El Cenozoico tardío continental de la provincia de Buenos Aires. In: de Barrio, R.E., Caballé, M.F., Llambías, E. (Eds.), Geología y recursos minerales de la Provincia de Buenos Aires. Relatorio del 16° Congreso Geológico Argentino, La Plata, pp. 139–158.